

## Neonatal Mice Spinal Cord Interneurons Send Axons through the Dorsal Roots

Laura Paulina Osuna-Carrasco<sup>3</sup>, Sergio Horacio Dueñas-Jiménez<sup>1</sup>, Carmen Toro-Castillo<sup>3</sup>,  
Braniff De la Torre<sup>3</sup>, Irene Aguilar-García<sup>5</sup>, Jonatan Alpírez<sup>1</sup>, Luis Castillo<sup>2</sup>  
and Judith Marcela Dueñas-Jiménez<sup>4\*</sup>

<sup>1</sup>Department of Neuroscience, CUCS, University of Guadalajara, Guadalajara 44340, <sup>2</sup>Basic Center, Autonomous University of Aguascalientes, Aguascalientes 20131, <sup>3</sup>Department of Translational Bioengineering, CUCEI, University of Guadalajara, Guadalajara 44430, <sup>4</sup>Department of Physiology, CUCS, University of Guadalajara, Guadalajara 44340, <sup>5</sup>Department of Molecular and Genomics, CUCS, University of Guadalajara, Guadalajara 44340, México

Spontaneous interneuron activity plays a critical role in developing neuronal networks. Discharges conducted antidromically along the dorsal root (DR) precede those from the ventral roots (VR) motoneurons. This work studied whether spinal interneurons project axons into the neonate's dorsal roots. Experiments were carried out in postnatal Swiss-Webster mice. We utilized a staining technique and found that interneurons in the spinal cord's dorsal horn send axons through the dorsal roots. *In vitro* electrophysiological recordings showed antidromic action potentials (dorsal root reflex; DRR) produced by depolarizing the primary afferent terminals. These reflexes appeared by stimulating the adjacent dorsal roots. We found that bicuculline reduced the DRR evoked by L5 dorsal root stimulation when recording from the L4 dorsal root. Simultaneously, the monosynaptic reflex (MR) in the L5 ventral root was not affected; nevertheless, a long-lasting after-discharge appeared. The addition of 2-amino-5 phosphonovaleric acid (AP5), an NMDA receptor antagonist, abolished the MR without changing the after-discharge. The absence of DRR and MR facilitated single action potentials in the dorsal and ventral roots that persisted even in low Ca<sup>2+</sup> concentrations. The results suggest that firing interneurons could send their axons through the dorsal roots. These interneurons could activate motoneurons producing individual spikes recorded in the ventral roots. Identifying these interneurons and the persistence of their neuronal connectivity in adulthood remains to be established.

**Key words:** Spinal cord interneurons, Antidromic activity, Dorsal root reflex, Monosynaptic reflex

### INTRODUCTION

Interneurons sending axons via the DR in the spinal cord produce antidromic action potentials regulating different types of peripheral receptors [1]. Possible controlling pain, other sensorial modalities, or muscle spindle activity [2]. Spontaneous firing and occasional bursting occurred in the dorsal roots (DR) after elevat-

ing the extracellular potassium concentration in isolated neonatal rat spinal cords [3]. This firing occurred with primary afferent depolarizations and antidromic discharges of nerve impulses in DR fibers [3, 4]. Antidromic activity has been observed in the dorsal root ganglia in chronically axotomized rats [5], and it can block or affect orthodromic impulses colliding with incoming afferent volleys [3, 6]. Stimulation of the ventral funiculus evoked antidromic discharges in the dorsal roots of neonatal rats *in vitro* (0~5-day old). The discharges were caused by the underlying afferent terminal depolarization reaching the firing threshold [7].

Some interneurons send their axons through the dorsal sensory fibers and the ventral pathways [8]. However, it is not known whether spinal interneurons produce antidromic and orthodrom-

Submitted June 18, 2021, Revised March 2, 2022,  
Accepted March 19, 2022

\*To whom correspondence should be addressed.  
TEL: 52-3310585313, FAX: 52-3310585200  
e-mail: mduenas@cucs.udg.mx

ic potentials in the neonatal spinal cord. In this work, we studied the presence of DR and VR spikes after abolishing the monosynaptic reflex and the DRR using bicuculline, a GABA antagonist drug, and the glutamic antagonist AP5 respectively.

Previous studies showed changes in soma size and number of neurons during development in rats [9], another purpose in this study was to determine whether these changes also occurred at this development stage in the mouse.

## MATERIALS AND METHODS

### *Subjects*

The experiments were conducted in 10 Swiss-Webster mice housed at room temperature with 12-hour light-dark cycles. Experimental protocols and animal care followed the NIH guidelines (USA) and were approved by the Institutional Ethics Committee in the Health Science Research Center under the Mexican Official Norm (NOM-062-ZOO-1999).

Animals at 2 to 13 postnatal days were anesthetized by methoxyflurane inhalation and then decapitated. After a ventral laminectomy, we used a tungsten needle to perform a longitudinal hemisection of the isolated spinal cords, keeping the ventral and dorsal roots between the T6 and the sacral spinal cord segments [10-12]. One hemicord was placed in a Sylgard silicone elastomer tube at the bottom of a recording chamber. The hemicord was perfused with oxygenated ACSF flowing at 10~14 ml/min. The bath solutions in flowed ACSF through a servo-controlled heater (TC-324B, Warner instruments) for temperature monitoring.

### *Fluorescent labeling*

We analyzed the presence of axons and their interneurons with fluorescent markers applied in the L4-L5 dorsal roots. For interneuron retrograde labeling, we used fluorescent dextran-amines (Molecular Probes, Eugene, Ore.), including rhodamine dextran amine (RDA, MW 3000) and fluorescein dextran-amine (FDA, MW 10 000).

In most cases, we used RDA and FDA at 50%. By mixing the markers we assured that the interneurons were marked correctly, thereby avoiding an RDA transsynaptic flow leak or insufficient FDA traveling antidromically to afferent fiber terminals. In all experiments, we checked under the microscope that there were no RDA nor FDA leaks in the bath solution or the spinal cord tissue. If so, the experiment was discarded.

We labeled DR afferent fibers by applying FDA, RDA, or the mixture of both fluorochromes to the cut L4 or L5 or both DRs. We also retrogradely labeled motoneurons by applying RDA and FDA to the L4-L5 ventral root. The markers were diluted in an

ACSF, 10 mmol/L solution, with 0.2% TritonX-100 (Sigma Chemical Co.). We employed fine suction electrodes pulled from polyethylene tubing (PE-190, Clay Adams, Parsippany, NJ.) and used negative pressure to introduce the roots into the tubes producing a tight seal, avoiding any fluorescent marker leakage. After 18-24 hours, the spinal cord was fixed by immersion in 4% PFA in a 0.1% phosphate buffer (7.4 pH) overnight. After ascending sucrose concentrations for cryoprotection, the spinal cords were sectioned in coronal slices on a freezing microtome. Tissue sections were placed on slides, dehydrated in ascending alcohol concentrations, cleared with Xylene, and covered with an antifade mounting medium (Vectashield, Vector Laboratories Inc. Burlingame, CA). We examined the tissue sections with an inverted Zeiss microscope and a laser scanning confocal imaging System (LSM 510). We analyzed the morphology and synaptology of interneurons, motoneurons, and afferent fibers in reconstructed three-dimensional arrangements from images containing several Z planes optical sections with the Zeiss LSM 510 software.

### *Stimulation and recording*

We placed the L4-L5 dorsal and ventral roots into the polyethylene suction electrodes for either stimulation or recording.

We evoked the MR and DRR in the afferent fibers by stimulating the dorsal root filament at the L5 segment, with ten pulse trains (0.5 ms each pulse) in two minutes. We recorded the MR at the L5 ventral root segment and the DRR at the L4 or L5 dorsal root. Some experiments were made in low calcium concentrations.

### *Data acquisition*

The signals obtained from the recording suction electrodes on DR and VR were amplified with Cyberamp 380 amplifiers (axon instruments: bandpass filtered between 10~10,000 Hz) and digitalized at 10 kHz with 16 bits resolution A/D converter (National Instruments NBIO-16). We used NIH institute software packages for data analysis.

### *Pharmacology*

Drugs were added using a gravity-feedline into the recording chamber (flow rate: 10~14 ml/min). We used the 2-amino-5-phosphonovaleric acid (AP5, 100  $\mu$ M) to block the monosynaptic response and Bicuculline methiodide (10~20  $\mu$ M) was administered for DRR inhibition. The halved spinal cord was placed in the chamber containing: 1) ACSF: 128 NaCl mM, 4 KCl mM, 2 CaCl mM, 1 MgSO<sub>4</sub> mM, 0.5 NaH<sub>2</sub>PO<sub>4</sub> mM, 25 NaHCO<sub>3</sub> mM, 30 mM Glucose; 2) ACSF with low calcium concentration (0.8 mM) and 1 Mg mM; 3) ACSF with bicuculline 2~5  $\mu$ M or, and 4) A solution with bicuculline 2  $\mu$ M and 2-amine 5-phosphonovaleric acid

(AP5). These solutions were continuously perfused with oxygen.

### Statistical analysis

In two experiments, we measured the size of the neuron soma in the ventral horn at 2 and 13 postnatal days (P2,  $n=15$ , and P13,  $n=27$ ). A linear regression analysis established the average size of the soma (Sigma-Plot software v11). At P2 was  $2,022 \mu\text{m}^3$  and at P13 was  $7,578 \mu\text{m}^3$ . Normality tests (Shapiro-Wilk) in P2 showed great variability and failed. To compare the difference between the soma size average value, we separate P13 group values under average ( $n=9$ ) and compare with P2. We performed a Mann-Whitney Rank Sum Test, where the P2 group and P13 under average equal variance test passed.

## RESULTS

### Neuron labeling

We analyzed the fluorescent marker patterns in all the spinal cords ( $n=10$ ). The RDA application to the L4 dorsal root produced the red fluorescent staining in afferent fibers. First-order interneurons were marked by the RDA close to the terminal branches due to a lower molecular weight (Fig. 1A). Application of FDA (green) in the L5 dorsal root only marked afferent fibers. RDA and FDA

mixture marked some interneurons in red when close to RDA afferent fibers (Fig. 1B, indicated by arrows). RDA and FDA mixture produced yellow staining. We only considered interneurons sending their axon by the dorsal roots when stained in yellow or green. Yellow-marked interneurons were found in the dorsal horn or the intermediate nucleus (Fig. 1C, 1D and Fig. 2A).

To locate these interneurons, we marked some spinal cord DRs exclusively with FDA. Most of the afferent fiber ended in the dorsal horn intermediate nucleus (Fig. 2A, a group of green-stained interneurons). In other cases, we retrogradely marked some interneurons with FDA in L5 and localized interneurons in the dorsal horn (Fig. 2B). These interneurons seemed to project their axons through the dorsal roots.

With the FDA and RDA mixture applied to L4 and FDA to L5 dorsal roots, we found yellow marked interneurons close to the intermediate nuclei region (Fig. 2C). Their morphology is different from motoneurons stained by the fluorochrome mixture applied in the L5 ventral root (Fig. 3B).

In our experiments, spinal interneurons sent axons through the dorsal roots. We localized most of these interneurons close to the intermediate nucleus and displayed several shapes, which differ from motoneurons.

Here, we did not study the dendritic arborizations nor their

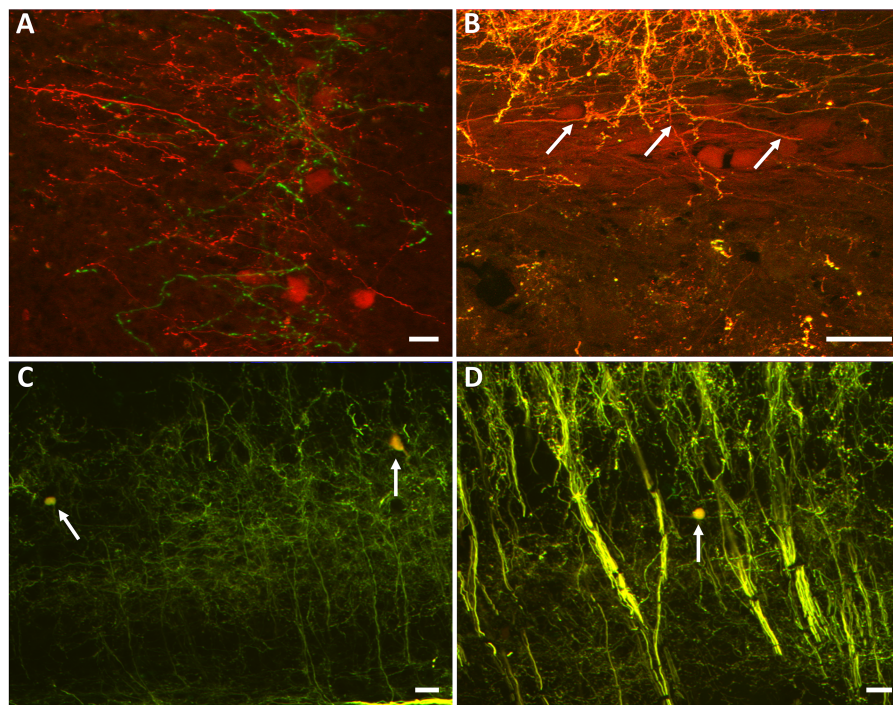


**Fig. 1.** L4-L5 spinal cord segments with fluorescent markers applied in dorsal roots. (A) RDA administered in L4 and FDA in L5. RDA leakage stained some interneurons in red (scale bar= $10 \mu\text{m}$ ). (B) Afferent fibers marked by FDA and RDA mixture in L5 dorsal root. The arrows indicate a red-stained fiber, close to it some interneurons marked in red (scale bar= $10 \mu\text{m}$ ). (C, D) Terminal afferent fibers in the dorsal spinal cord, the arrows indicate small neurons stained in yellow (scale bar= $10 \mu\text{m}$ ).

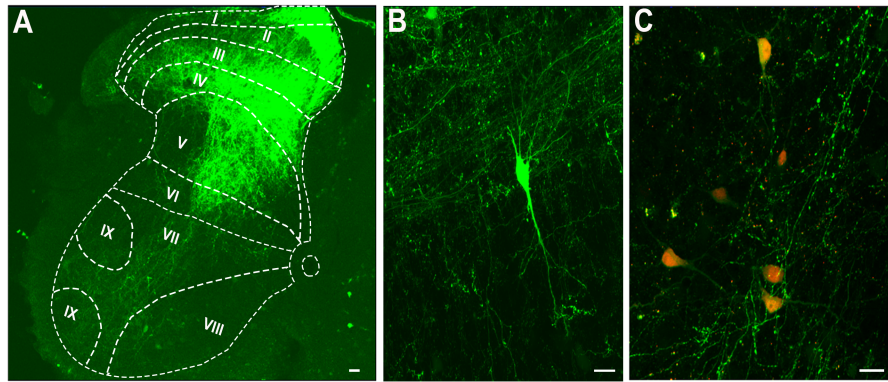


**Fig. 2.** L4-L5 spinal cord segments with fluorescent markers. (A) FDA afferent fiber (scale bar, 100  $\mu$ m). Note a limited number of afferent fibers in the spinal cord ventral horn (the Rexed-laminae schematic superimposed). (B) A FDA single marked interneuron. The FDA in the L5 dorsal root (scale bar=10  $\mu$ m). (C) FDA and RDA mixture applied in L4 dorsal root and FDA in the L5 dorsal root. Several interneurons were stained in an orange hue (scale bar=10  $\mu$ m). In A, B, and C, different spinal cord tissues are shown.

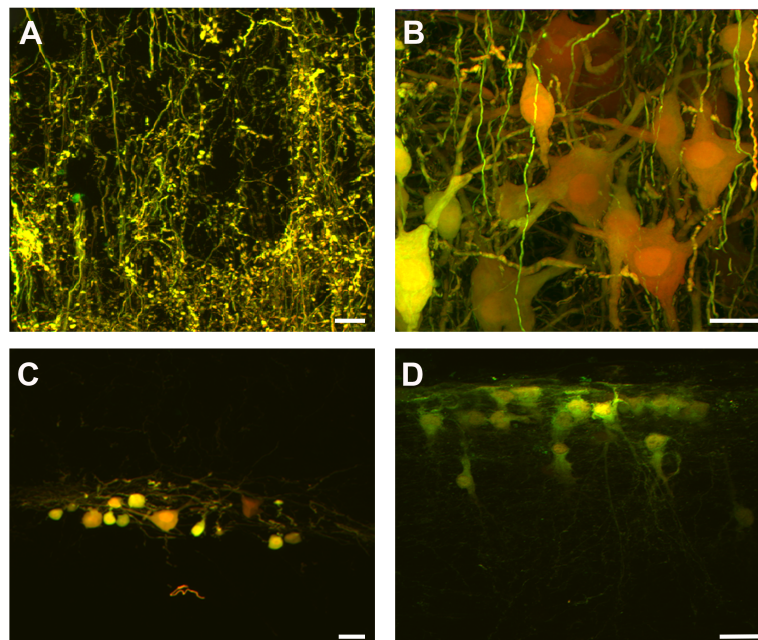


**Fig. 3.** Images of the spinal cord in L4-L5 segments with the mixture of RDA and FDA fluorescent markers. (A) Terminal afferent fibers arriving at the ventral spinal cord were stained by applying the fluorescent mixture in the L5 dorsal root (scale bar, 10  $\mu$ m). (B) The mixture was administered through the L5 ventral and dorsal root. It is important to note that the motoneurons and the afferent fiber arriving at the motor nucleus were stained (scale bar, 50  $\mu$ m). (C) Neurons traveling grouped on the spinal cord dorsal surface. (D) The neurons were penetrating a deep region in the spinal cord.

changes with age, as assessed in previous studies. In a developing stage, Westerga & Gramsbergen observed a considerable increase in motoneuron soma size in rats, different distribution patterns, and longer and more extensive arborizations in the cervical region in comparison to the lumbar region [9]. These temporal and spatial differences may influence motor development in a rostrocaudal manner [13]. Dendrite bundles appeared relatively late in the Soleus motoneuron compared to the Tibial anterior; this is related to the fine-tuning of neuronal activity, rather than patterning of

motor activity [9].

The afferent fibers arriving at the motor nucleus exhibited a bulb-like terminal when we applied the fluorochrome mixture into the dorsal roots (Fig. 3A). With FDA, fibers were marked in green (Fig. 3B). The mixture in L5 VR stained neurons and revealed the motoneuron morphology. However, no interneurons were marked in this ventral motor region. In addition, the fluorochrome mixture marked some cells that resembled neurons traveling in groups on the spinal cord dorsal surface (Fig. 3C). Thereafter, they penetrated

the deep layers of the spinal cord (Fig. 3D).

In these experiments, we have observed no fluorochrome leaks, the neurons on the intermediate nucleus were marked in yellow and the fibers in green (Fig. 2C). On the other hand, the clustered cells found in the spinal cord's dorsal surface were marked in yellow (Fig. 3C, 3D).

We found some cells traveling in the spinal cord dorsal surface. We did not know if these cells were neurons, glia, or stem cells. This could be studied using markers for glia, neurons, or stem cells. As we noticed cells traveling in groups in the dorsal horn surface of the mouse spinal cord, they could be identified immunohistologically in further studies. It could reveal the type of cells and clarify if some of them are progenitor neurons [14-16].

In a developmental study in kittens, the volume of the lateral cervical nucleus and the glial cells increased sixfold during a 120-day observation, the volumes of myelinated axons also increased [17]. Probably genetic strategies could confirm whether these interneurons remain in adulthood and what is their function.

### Discharges in the dorsal and ventral roots

With the stimulation of the L5 dorsal root in 10-day old mice ( $n=4$ ), we took control of the monosynaptic reflex in the L5 ventral root and the DRR in the L4 dorsal root (Fig. 4A). The recordings obtained appeared similar in all the experimental subjects.

After control recordings, a bath with bicuculline (10~20  $\mu\text{M}$ ) eliminated DRR but not the monosynaptic reflex (Fig. 4B). Interestingly, a long latency reflex occurred after the bicuculline application in the ventral root (Fig. 4B, indicated by an arrow). Similar activity has been observed in spinal cord motor neurons in the turtle in the presence of bicuculline [18].

AP5 and bicuculline application decreased MR and DRR after a few minutes (Fig. 4C, 4D). We recorded sporadic action potentials in the DR (Fig. 4C, 4D, second traces).

After washing out bicuculline and AP5, the normal MR and DRR were reestablished (Fig. 4E, indicated by arrows in the two traces). A low  $\text{Ca}^{2+}$  solution was then applied and MR, DRR, and after discharge disappeared; interestingly, almost simultaneous

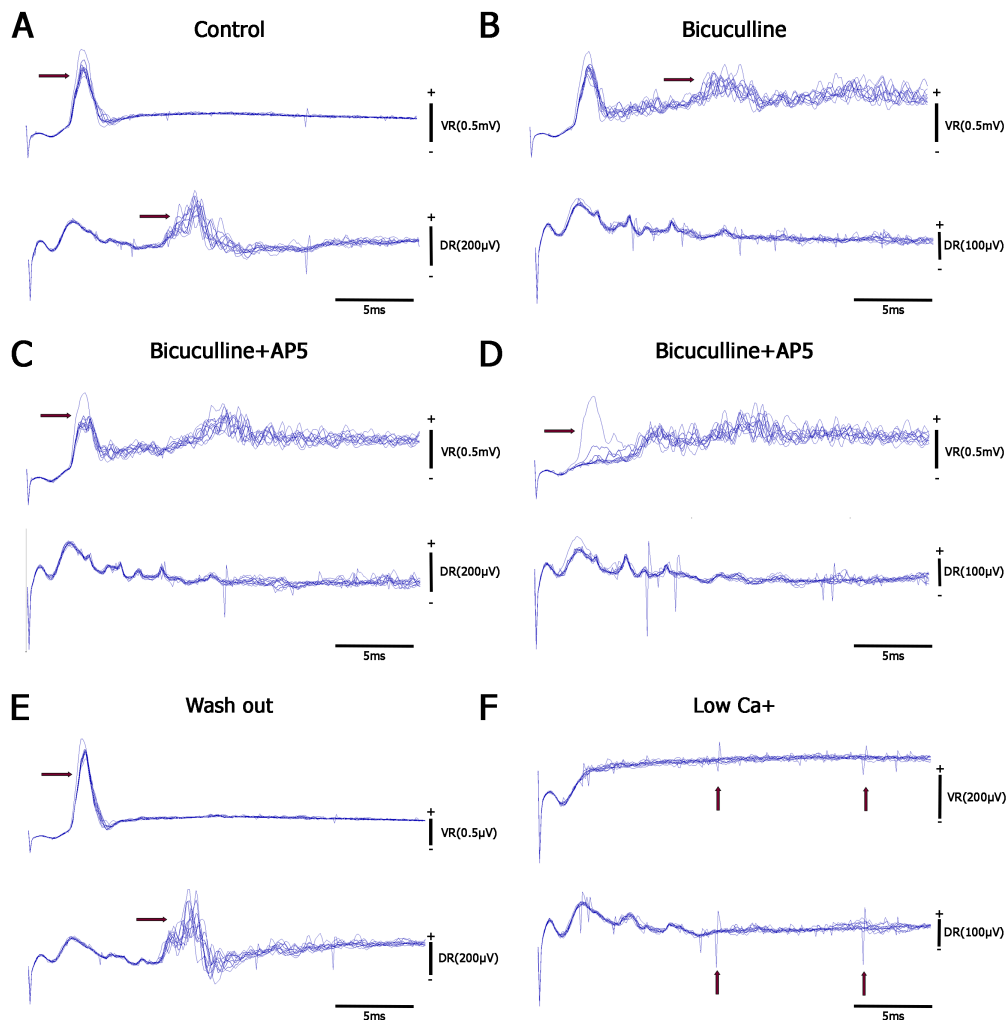


**Fig. 4.** DRR and MR recordings in the lumbar spinal cord. MR and DRR control recordings in L5 ventral and L4 dorsal roots, respectively (indicated by arrows, upper and lower traces in (A) aCSF control, (B) aCSF with bicuculline (10~20  $\mu\text{M}$ ). C and D illustrate MR and DRR in the presence of bicuculline plus AP5 (100  $\mu\text{M}$ ). MR depression began 2~4 min after applying AP5. Note that most of the MR was almost fully eliminated, but DR action potentials still appeared (C, D), lower traces. (E) Dorsal and ventral root reflexes recovered after drug washout. (F) VR and DR recording under low  $\text{Ca}^{2+}$ , the ventral and dorsal roots reflexes were eliminated, but spiking persisted (indicated by arrows).

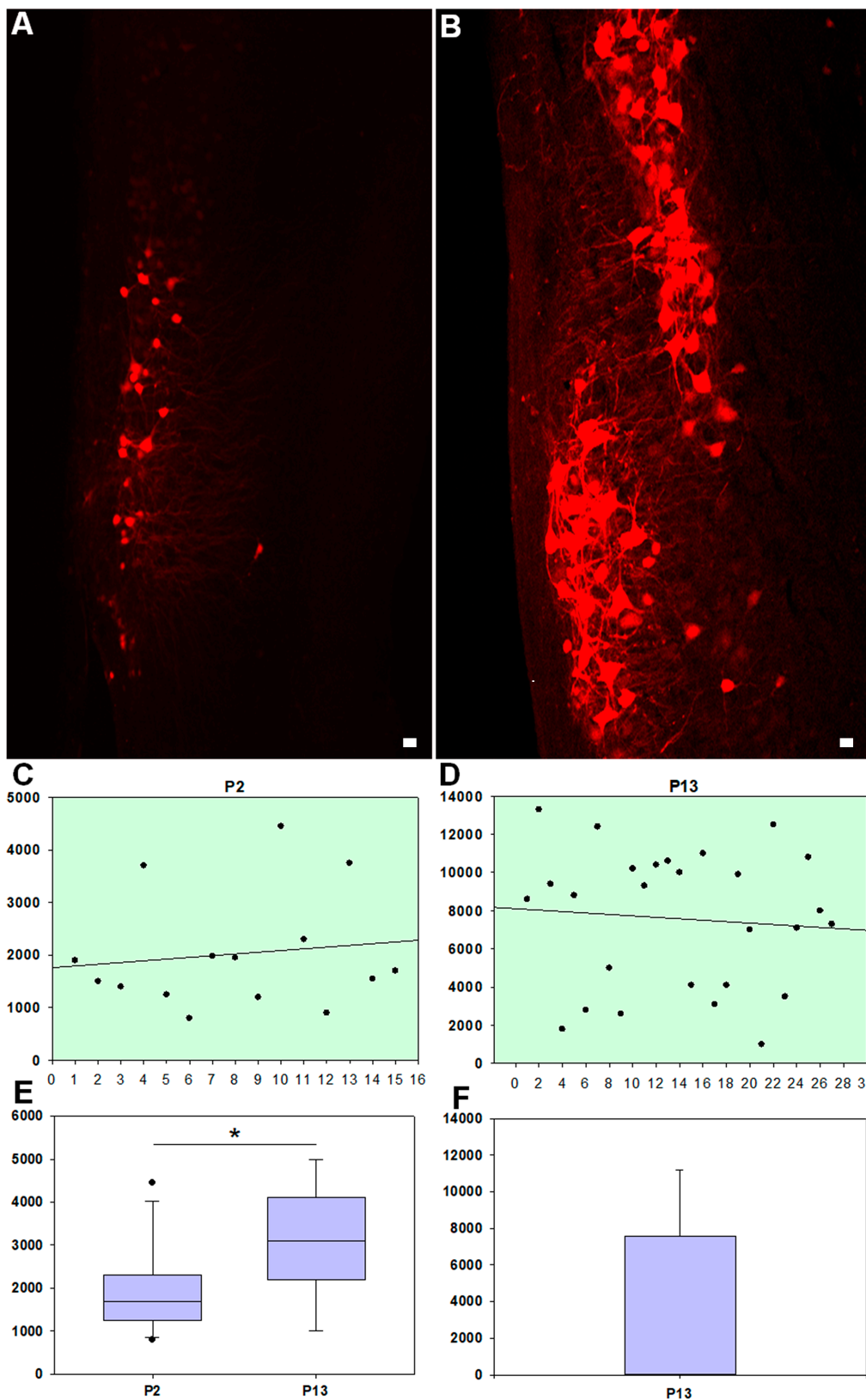


**Fig. 5.** Nuclei formation in the ventral horn. (A) At Postnatal day 2, a few neurons were stained with RDA. (B) At postnatal day 13, two nuclei were identified. (C, D) The neurons in both nuclei were also segregated by size (under and above-average value, described in methods). The number of neurons is in the abscissa and the size in cubic micrometers in the ordinate. The line in the graphs indicates linear regression. (E) Comparing the size in P2 and P13 neurons under linear regression (average value). Note that in the P2, the size of most of the neurons is under 2,000  $\mu\text{m}^3$ . At P13; there was a statistically significant increase in the size and number of neurons ( $p < 0.05$ ). (F) The mean value of neuron size in both nuclei at P13 increased up to four times.

action potentials were observed in the VR and the DR (Fig. 4F, indicated by arrows in the two traces).

In these experiments, spontaneous activity of interneurons was demonstrated in both roots, dorsal and ventral, although it cannot be confirmed that they come from the same interneuron.

We did not verify whether the recorded interneurons produce activity (action potentials) traveling antidromically in the dorsal roots. However, we found antidromic activity in the dorsal roots even in the presence of bicuculline, AP5, and low calcium. In another study, 2~4 postnatal day mice presented depression curves that were not explained by presynaptic activation failure (suppressed by AP5). Low calcium concentration reduced the average amplitude and depression, and a higher calcium concentration increased both. Increasing the bath temperature from 24 to 32 Celsius produced a small change in amplitudes, but the depression was reduced noticeably at most frequencies [19]. Therefore, these AP could be generated by the interneurons when their axons are sufficiently depolarized. Thus, an antidromic activity could have a different origin than PAD, and consequently, other functions. On the other hand, ephaptic interaction in afferent fibers could also produce antidromic firing [20, 21].

In the neonatal rat, spinal cord neurons firing antidromic bursts have been observed [7]. Potassium transient effects are not restricted to the developing spinal cord and also occur in adulthood [4, 5]. Therefore, it is of our interest to investigate whether they remains in adult mice.

Antidromic spike function in the dorsal roots could participate in regulating activity in the afferent inflow of information related to inflammation and pain. DRR in afferent fibers raises the hypothesis that whether mediated antidromic activity contributes to neurogenic inflammation [22]. Sectioning the sciatic nerve of neonatal rats triggers the growth of afferent fiber in the VR, and stimulation in the L5 spinal cord evoked long latency antidromic potentials in the L5's ventral root. However, in normal rats, such potentials rarely appeared [23].

Neurons of the dorsal reticular nucleus in the cat showed sub-threshold oscillatory activity leading to the generation of cumulative excitation (windup), in response to low-frequency C-fiber afferent input and low frequency depolarizing currents. Dorsal reticular nucleus cells send collateral branches to the spinal cord, that could regulate pain-related motor responses, and ascending nociceptive information via descending fibers ending at the spinal dorsal horn [24]. In rodents, this nucleus is part of a reticular-spinal-reticular circuit through its reciprocal connections with the spinal dorsal horns superficial and deep laminae [25-28]. Other studies suggest the involvement of the dorsal reticular nucleus with the modulation of ascending nociceptive information from

the spinal dorsal horn in this species [29, 30].

We found one nucleus with small-sized neurons at P2 and two nuclei at P13 (Fig. 5A, 5B). Fig. 5C, 5D illustrate all neurons stained in P2 (n=15) and P13 (n=27) in lumbar spinal cord sagittal slices. The difference in the median values between the two groups (P2 and P13 <average value, n=9) are statistically significant (p=0.049). In P2 this value was 1,700  $\mu\text{m}^3$  and in P13 was 3,100  $\mu\text{m}^3$  (Fig. 5E).

Developing serotonergic motoneuron innervation is related to the postnatal development of motor functions already recognized in the second postnatal week [13]. In our study, we found a significant neuronal soma size increase at a similar postnatal age. Marked neurons are not of the same type or from a specific neuron group. That could refer to a different organization of the activation pattern. It will be of great interest to know whether some of these neurons are GABAergic, if so, they could be associated with PAD interneurons related to DRR. It is possible that an increase in the motoneuron pool relocate some interneurons to a dorsal region in the spinal cord.

We used the double labeling to identify interneurons with axons in the dorsal roots through the Fluorescent dextran-amines technique developed in the nervous system of the chicken embryo [31]. The presence and location of these interneurons in the spinal cord of the adult mice and their functional role should be studied to elucidate the functional connections in adulthood.

## ACKNOWLEDGEMENTS

I would like to thank Dr. Robert E. Burke since some of the data presented here were previously obtained under the assistance of Dr. Robert Burke at NIH. He taught me the mouse preparation and histological staining, as well as the use of confocal microscopy. These data files have not been presented or analyzed previously. And thanks to Dr. JR López-Ruiz at Michigan University for his assistance in the manuscript.

## REFERENCES

1. Dubuc R, Rossignol S (1989) The effects of 4-aminopyridine on the cat spinal cord: rhythmic antidromic discharges recorded from the dorsal roots. *Brain Res* 491:335-348.
2. Martín M, Béjar J, Chávez D, Ramírez-Morales A, Hernández E, Moreno L, Contreras-Hernández E, Glusman S, Cortés U, Rudomin P (2019) Supraspinal shaping of adaptive transitions in the state of functional connectivity between segmentally distributed dorsal horn neuronal populations in response to nociception and antinociception. *Front Syst*

- Neurosci 13:47.
3. Kremer E, Lev-Tov A (1998) GABA-receptor-independent dorsal root afferents depolarization in the neonatal rat spinal cord. *J Neurophysiol* 79:2581-2592.
  4. Lothman EW, Somjen GG (1976) Reflex effects and post-synaptic membrane potential changes during epileptiform activity induced by penicillin in decapitate spinal cords. *Electroencephalogr Clin Neurophysiol* 41:337-347.
  5. Russell LC, Burchiel KJ (1988) Spontaneous activity in afferent and efferent fibers after chronic axotomy: response to potassium channel blockade. *Somatosens Mot Res* 6:163-177.
  6. Wójcik G, Lupa K, Niechaj A (1992) Pattern of irregular dorsal root discharge in the spinal cat. *Arch Int Physiol Biochim Biophys* 100:197-201.
  7. Vinay L, Brocard F, Fellippa-Marques S, Clarac F (1999) Antidromic discharges of dorsal root afferents in the neonatal rat. *J Physiol Paris* 93:359-367.
  8. Coggeshall RE (1979) Afferent fibers in the ventral root. *Neurosurgery* 4:443-448.
  9. Westerga J, Gramsbergen A (1992) Structural changes of the soleus and the tibialis anterior motoneuron pool during development in the rat. *J Comp Neurol* 319:406-416.
  10. Jovanovic K, Burke RE (2004) Anatomical organization of motoneurons and interneurons in the mudpuppy (*Necturus maculosus*) brachial spinal cord: the neural substrate for central pattern generation. *Can J Physiol Pharmacol* 82:628-636.
  11. Jovanovic K, Burke RE (2004) Morphology of brachial segments in mudpuppy (*Necturus maculosus*) spinal cord studied with confocal and electron microscopy. *J Comp Neurol* 471:361-385.
  12. Li Y, Brewer D, Burke RE, Ascoli GA (2005) Developmental changes in spinal motoneuron dendrites in neonatal mice. *J Comp Neurol* 483:304-317.
  13. Takahashi S, Tanaka H, Oki J (1999) Development of spinal motoneurons in rats after a neonatal hypoxic insult. *Pediatr Neurol* 21:715-720.
  14. Hao Z, Yeung J, Wolf L, Doucette R, Nazarali A (1999) Differential expression of Hoxa-2 protein along the dorsal-ventral axis of the developing and adult mouse spinal cord. *Dev Dyn* 216:201-217.
  15. Gleeson JG, Lin PT, Flanagan LA, Walsh CA (1999) Doublecortin is a microtubule-associated protein and is expressed widely by migrating neurons. *Neuron* 23:257-271.
  16. Helms AW, Johnson JE (2003) Specification of dorsal spinal cord interneurons. *Curr Opin Neurobiol* 13:42-49.
  17. Broman J, Flink R, Westman J (1987) Postnatal development of the feline lateral cervical nucleus: I. A quantitative light and electron microscopic study. *J Comp Neurol* 260:539-551.
  18. Bautista W, Aguilar J, Loeza-Alcocer JE, Delgado-Lezama R (2010) Pre- and postsynaptic modulation of monosynaptic reflex by GABA<sub>A</sub> receptors on turtle spinal cord. *J Physiol* 588(Pt 14):2621-2631.
  19. Li Y, Burke RE (2001) Short-term synaptic depression in the neonatal mouse spinal cord: effects of calcium and temperature. *J Neurophysiol* 85:2047-2062.
  20. Jiménez I, Rudomin P, Solodkin M, Vyklicky L (1983) Specific and potassium components in the depolarization of the Ia afferents in the spinal cord of the cat. *Brain Res* 272:179-184.
  21. Bolzoni E, Jankowska E (2019) Ephaptic interactions between myelinated nerve fibres of rodent peripheral nerves. *Eur J Neurosci* 50:3101-3107.
  22. Lin Q, Zou X, Willis WD (2000) Adelta and C primary afferents convey dorsal root reflexes after intradermal injection of capsaicin in rats. *J Neurophysiol* 84:2695-2698.
  23. Chung BS, Sheen K, Chung JM (1991) Evidence for invasion of regenerated ventral root afferents into the spinal cord of the rat subjected to sciatic neurectomy during the neonatal period. *Brain Res* 552:311-319.
  24. Soto C, Canedo A (2011) Intracellular recordings of subnucleus reticularis dorsalis neurones revealed novel electrophysiological properties and windup mechanisms. *J Physiol* 589:4383-4401.
  25. Villanueva L, de Pommery J, Menétrey D, Le Bars D (1991) Spinal afferent projections to subnucleus reticularis dorsalis in the rat. *Neurosci Lett* 134:98-102.
  26. Villanueva L, Le Bars D (1995) The activation of bulbo-spinal controls by peripheral nociceptive inputs: diffuse noxious inhibitory controls. *Biol Res* 28:113-125.
  27. Almeida A, Tavares I, Lima D (2000) Reciprocal connections between the medullary dorsal reticular nucleus and the spinal dorsal horn in the rat. *Eur J Pain* 4:373-387.
  28. Almeida A, Størkson R, Lima D, Hole K, Tjølsen A (1999) The medullary dorsal reticular nucleus facilitates pain behaviour induced by formalin in the rat. *Eur J Neurosci* 11:110-122.
  29. Lima D, Almeida A (2002) The medullary dorsal reticular nucleus as a pronociceptive centre of the pain control system. *Prog Neurobiol* 66:81-108.
  30. Monconduit L, Desbois C, Villanueva L (2002) The integrative role of the rat medullary subnucleus reticularis dorsalis in nociception. *Eur J Neurosci* 16:937-944.
  31. Glover JC, Petursdottir G, Jansen JK (1986) Fluorescent dextran-amines used as axonal tracers in the nervous system of the chicken embryo. *J Neurosci Methods* 18:243-254.